Magnetic and melting transitions of oxygen monolayers and multilayers physisorped on exfoliated graphite

Youichi Murakami* and Hiroyoshi Suematsu
Department of Physics, Faculty of Science, University of Tokyo, Hongo 7-3-1, Bunkyo-ku, Tokyo 113 Japan
(Received 12 June 1995; revised manuscript received 16 February 1996)

The magnetic susceptibility (χ) and magnetization of oxygen (O_2) monolayers and multilayers physisorped on exfoliated graphite have been investigated in order to elucidate the magnetic and melting transitions in the two-dimensional (2D) system. An anisotropy of χ in the dense monolayer phase has been observed below $T_N = 11.9 \pm 0.1$ K. The magnetization process shows the precursor of the spin-flop transition, which is estimated to occur in the magnetic-field region $6 < H < 7$ T at $T = 5.0$ K. These experimental results confirm the existence of magnetic long-range order below T_N. The exchange field between nearest-neighbor O_2 molecules in a monolayer is estimated as 70% of that of bulk O_2. The anisotropy in the fluid-II phase has also been observed, which means that O_2 molecules in this phase have orientational order. In the bilayer region, the second O_2 layer is not only ordered magnetically, but the magnetic ordering of the first layer is also destroyed in a magnetic field when the second layer coverage exceeds 65% of the full coverage of the second layer. These results are discussed in relation to a random-exchange field effect between the first and second layers, which are incommensurate to each other. The feature of melting transitions in the multilayer region is described in terms of surface melting. [S0163-1829(96)03430-3]

I. INTRODUCTION

Oxygen is a unique gas which has the spin $S = 1$ and becomes a magnetic insulator in the condensed phase. Because of the direct-exchange interaction between molecules, the bulk solid of O_2 undergoes a transition to an antiferromagnetic ordered state below 23.9 K. The interaction is considered to be Heisenberg-like.[1,2] The easy axis of the spin is perpendicular to the molecular axis whose small anisotropy comes from the anisotropy of the molecular orbit.[3,4] O_2 molecules physisorped on graphite grow in a layer-by-layer fashion[5,6] and have a two-dimensional (2D) incommensurate lattice referred to the graphite lattice. So, we can expect to get an ideal substance to study a 2D Heisenberg antiferromagnetic spin system.

In the last two decades this system has been extensively investigated by many experimental methods, namely, x-ray diffraction (XRD),[7–10] neutron diffraction (ND),[11–16] susceptibility (χ),[17–21] heat capacity,[22–25] low-energy electron diffraction (LEED),[26–29] reflection high-energy electron diffraction (RHEED),[30,31] electron energy-loss spectroscopy (EELS),[32–34] photoelectron spectroscopy (XPS and UPS),[35–37] resonance electron scattering (RES),[38,39] near-edge x-ray-absorption fine structure (NEXAFS)[40] and many theoretical works.[41–47] From the structural studies it was found that this system has many phases depending on temperature and O_2 coverage C. The coverage $C = 1$ is defined in this paper so as to form the triangular $\sqrt{3} \times \sqrt{3}$ superlattice referred to the graphite lattice. In a simplified phase diagram of the monolayer, there are two principal phases, the dilute δ and dense ε and ζ phases, whose molecular axes are, respectively, parallel and perpendicular to the graphite surface.

The studies of magnetic properties of O_2 monolayers have been pioneered by Nielsen and McTague.[11,12] In ND experiments they revealed the structural phase transition of the ζ phase to a deformed triangular lattice, ε phase, and identified it as an antiferromagnetic phase. The magnetic distortion was also observed in XRD measurements.[9] Recently, we have observed more clearly the antiferromagnetic Bragg peak of the ε phase by ND measurements[15,16] and an anomaly of χ at $T_N = 11.9 \pm 0.1$ K.[20,21] However, any anisotropy of χ could not be observed below T_N. In the LEED measurements the magnetic transition was also not observed at the temperature.[27,29]

In this paper, we report a more detailed χ measurement and magnetization process focusing on the magnetic phase transitions of the mono- and bilayer regions. Here, we have observed the difference between χ in the direction parallel and perpendicular to the spin axis below T_N. The perpendicular susceptibility $\chi_\perp$ approximately agrees with a spin-wave theory for the 2D Heisenberg model. The high-field magnetization process shows the precursor of the spin-flop transition in the ε phase though the transition is not directly observed up to $H = 5.5$ T. These experimental results confirm the existence of the magnetic long-range order in the ε phase. An anisotropy of χ is also observed in the fluid-II phase. In the bilayer region, the second layer, which is the next-nearest-neighbor layer to the graphite surface, is not ordered magnetically though the first layer is ordered. In the coverage region $C > 2.8$, the magnetic ordering of the first layer at T_N also disappears. These results are discussed by a random field effect between the first and second layers. Finally, the melting features in the multilayer region are described, which are consistent with surface melting proposed by the previous ND experiments.[13,14]

II. EXPERIMENTAL PROCEDURE

Three types of exfoliated graphite have been tried as a substrate, i.e., Grafoil,[48] vermicular graphite,[49] and homemade exfoliated graphite which was made by a careful ex-

foliation from an HNO_3-graphite intercalation compound. We used Grafoil in the course of the present experiments because it has a large surface area and a good parallelism of the adsorption plane and its small in-plane coherence[50] did not affect the quality of the observed χ. The Grafoil was baked out at 800 °C for a week to remove adsorbed impurities. The surface area was measured by the Brunauer-Emmett-Teller (BET) method[51] with use of nitrogen gas. A coverage of an O_2 film was determined from the surface area of grafoil and the dose of O_2 gas.

The measurements of χ were carried out with a SQUID magnetometer. In order to obtain the net value of χ of the O_2 monolayer we must subtract the χ of Grafoil from the observed value for O_2 on Grafoil. The χ of Grafoil includes the diamagnetism of graphite and paramagnetic impurities (at a concentration of about 10^{18}/g), which give a much larger value than the O_2 monolayers. The weight of the Grafoil used in these experiments was about 50 mg, which has an effective surface area of about 1.2 m^2. A sample cell was made of Stycast No. 1266 which has a low concentration of magnetic impurities and does not generate noise from eddy currents. In order to exchange a sample easily, we used a soap seal as a vacuum seal.[52] The size of the sample space in the cell was 5 mm in diameter and 6 mm in length. The sample cell was connected with a pipeline which was led to a gas handling system. The pressure of O_2 gas was monitored by a diaphragm gauge.

The growth of the O_2 monolayers was carefully carried out as follows. The sample cell was cooled down to $T=54.5$ K and O_2 gas was introduced; the temperature was chosen just above the triple temperature ($T_3=54.35$ K) of bulk O_2 because the wetting transition occurs at T_3.[5,6] During the introduction of gas, the pipeline was heated in order to avoid condensation of bulk O_2 on any place other than the sample. The crystal growth was made by many steps of small doses of O_2 gas instead of one shot dose, otherwise we could not get good samples. Measurements of the equilibrium pressure at each dose gave us the isotherm curve, in which some steps could be obtained corresponding to the layer-by-layer growth. This isotherm curve was used for a confirmation of the quantity of adsorbed O_2. When the dose of the adsorbed O_2 reached a desired coverage, the sample cell was isolated from the gas handling system. Next, the sample was cooled down gradually and annealed for at least 30 min at the melting temperatures of the O_2 layer.

In the usual cases we applied a magnetic field and measured χ with increasing temperature. After measuring χ up to 50 K, we introduced the next dose of O_2 and repeated this process. The χ during cooling was measured sometimes to check the hysteresis of phase transitions. After all χ measurements had been done, the O_2 was completely desorbed at a high temperature ($T>100$ K), and the χ for Grafoil was measured again in order to check a change in χ for the background. In almost all the cases, the change in χ of the substrate was negligible, compared with χ of O_2 monolayers. We carried out the detailed χ measurements for the magnetic fields $H=0.05$, 0.5, and 1 T. The results were almost the same for all fields, so we show the data for $H=1$ T, which had the best statistics.

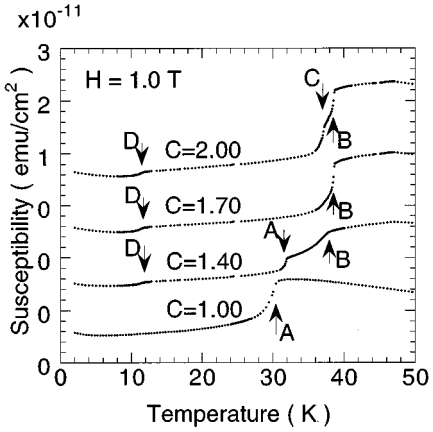

FIG. 1. Temperature dependence of $\chi(H\|S)$ of O_2 for different monolayer coverages in the direction of the field parallel to the Grafoil surface ($H=1$ T). The arrows A, B, C, and D indicate the melting temperature of the δ phase, the first layer, the second layer of the ξ phase, and the $\varepsilon-\zeta$ magnetic phase transition temperature.

III. EXPERIMENTAL RESULTS

A. Susceptibility of mono- and bilayer regions

Figure 1 shows the temperature dependence of the dc susceptibility $\chi(H\|S)$ parallel to the Grafoil surface for $C=1.00$, 1.40, 1.70, and 2.00, at $H=1$ T. Hereafter, $\chi(H\|S)$ and $\chi(H\perp S)$ stand for the χ with the magnetic field parallel and perpendicular to the Grafoil surface, respectively. The unit of the ordinate (emu/cm^2) means the absolute value of χ of O_2 per unit surface area of Grafoil. An anomaly of χ at $T=30.5\pm0.1$ K for $C=1.00$ (arrow A) corresponds to the melting transition of the δ phase. The change of χ at the melting temperature seems to be continuous: the precursory behavior is observed below the melting temperature. The arrow B at $T=38.4\pm0.1$ K for $C=1.40$ and 1.70 shows the melting temperature of the monolayer ζ phase. For $C=1.40$, the δ phase coexists with the ζ phase. The anomaly D at $T_N=11.9\pm0.1$ K indicates the $\varepsilon-\zeta$ antiferromagnetic phase transition. The definition of T_N and the detailed description of the $\varepsilon-\zeta$ transition is given in the next section. For $C=2.00$, χ shows a two-step change at 38.4 ± 0.1 and 39.0 ± 0.1 K denoted by the arrows C and B, respectively. These temperatures are considered the melting temperatures of first and second layers, respectively, as proposed by XRD measurements.[8,9] Namely, in the XRD model there is the η phase between these temperatures, which consists of a solid first layer and a fluid second layer. The coverage dependence of the changes of χ at $T=38.4$ and 39.0 K is consistent with this model as described later.

These temperatures of melting and magnetic transitions are consistent with the previous experimental results.[7–12,22–25] The melting temperature of the δ phase is increased from $T=25.5$ to 31.8 K as the coverage increases from $C=1.0$ to 1.2. The previous LEED experiments proposed the existence of a θ phase above the melting temperature of the δ phase, which is believed to be a 2D solid with molecular axis disorder.[29] However, we could not observe any evidence of the θ phase in the χ measurements. The melting temperature of monolayer ζ phase and the $\varepsilon-\zeta$ transition temperature have no coverage dependence. This means

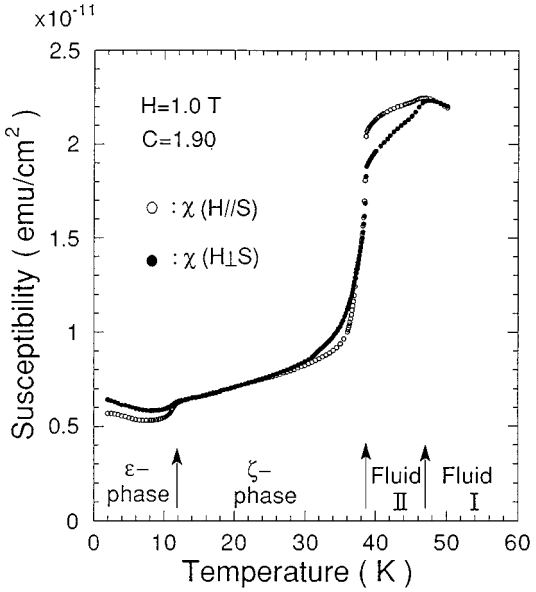

FIG. 2. Temperature dependence of $\chi(H\|S)$ and $\chi(H\perp S)$ of the dense O_2 monolayer ($C=1.90$) at $H=1.0$ T, which are denoted by open and closed circles, respectively.

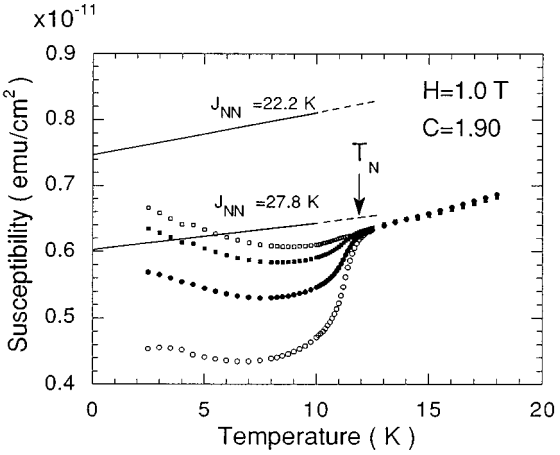

FIG. 3. Temperature dependence of χ of the dense O_2 monolayer ($C=1.90$) near the $\varepsilon-\zeta$ magnetic phase transition temperature at $H=1.0$ T. The $\chi(H\|S)$ and $\chi(H\perp S)$ are denoted by closed circles and squares, respectively. The open circles and squares indicate the parallel ($\chi_\|$) and perpendicular ($\chi_\perp$) susceptibility, respectively. The solid lines indicate the susceptibilities from a spin-wave theory of a 2D Heisenberg antiferromagnet in a square lattice, for $J_{NN}=27.8$ and 22.2 K.

the density of the ζ phase is not changed with coverage, which is consistent with the XRD experiments.[8] The LEED experiment reported previously two different monolayer phases in the ζ phase, that is, $\zeta1$ and $\zeta2$ phases and found the transition temperature at $T=18$ K between the $\zeta1$ and $\zeta2$ phases.[27] However, we could not observe any anomaly of χ in this temperature region. With increasing coverage ($C>3.2$) we detect a contamination of α and β phases of bulk O_2, the 3D antiferromagnetic and paramagnetic phases, respectively.

Figure 2 shows the temperature dependence of $\chi(H\|S)$ and $\chi(H\perp S)$ in the dense monolayer coverage region ($C=1.90$). The $\chi(H\|S)$ and $\chi(H\perp S)$ are denoted by open and closed circles, respectively. The temperature dependence of $\chi(H\perp S)$ is almost the same as that of $\chi(H\|S)$. However, there are two differences. One is the anisotropy of χ in the ε phase, that is described in the next section in detail. The second is the anisotropy of χ in fluid II. In previous works two kinds of fluid phases were reported, i.e., fluids I and II. Fluid I, which is a higher-temperature phase, is considered to be a normal liquid phase, while in fluid II a very broad peak was observed in the XRD measurement in this coverage region.[7,8,10] The structure of fluid II in this coverage region is not clear. The observed anisotropy of χ suggests at least that in fluid II the molecular axis does not have a random distribution though the translational symmetry may be almost lost. The anisotropy between 32 and 38 K in Fig. 2 is attributed to a small admixture of the δ phase for $\chi(H\perp S)$.

B. $\varepsilon-\zeta$ magnetic phase transition

Figure 3 shows the temperature dependence of $\chi(H\|S)$ and $\chi(H\perp S)$ around the $\varepsilon-\zeta$ magnetic phase transition at $C=1.90$. The $\chi(H\|S)$ and $\chi(H\perp S)$ are denoted by closed circles and squares, respectively. These χ show an anomaly at $T_N=11.9\pm0.1$ K, which is determined from an onset temperature of the separation of $\chi(H\|S)$ and $\chi(H\perp S)$. There are two important features; one is the anisotropy of χ below T_N, which directly indicates the existence of a long-range-order antiferromagnetic state in the ε phase,[53] the other is the continuous change of χ below T_N, which is in contrast to the usual first-order transition with lattice distortion. The open circles and squares in Fig. 3 denote $\chi_\|$ and $\chi_\perp$, which are the parallel and perpendicular χ to the spin direction, respectively. They are deduced from the observed $\chi(H\|S)$ and $\chi(H\perp S)$ by considering the random distribution of the crystal axis of the O_2 monolayer in the plane and the mosaic spread of the monolayer coming from the structure of Grafoil. Here, we do not take account of the tilt angle of the O_2 molecular axis proposed by the recent RES (Refs. 45 and 46) and NEXAFS (Ref. 47) experiments. If the molecular axis tilts, the effect should convolute with the mosaic effect of Grafoil.

The solid line in Fig. 3 indicates the calculated result for spin-wave theory in the case of a 2D Heisenberg antiferromagnet with a square lattice.[54] Here the interaction ($J_{NN}=27.8$ K) is deduced independently from the observed intermolecular distance between O_2 molecules in our recent ND measurements,[16] and the experimental distance dependence of the direct exchange energy obtained from the estimated exchange energy in some bulk O_2 phases [see Eq. (4)].[2] The theoretical value of χ agrees with the $\chi_\perp$ at a low-temperature region except for a small temperature dependence. This seems to show that the spin-wave theory is effective in the 2D system. However, the calculated curve for $J_{NN}=22.2$ K, which is deduced from the $\chi_\perp$ measurements, is not in good agreement compared with the χ for $J_{NN}=27.8$ K. The detailed discussion will be given in Sec. IV A.

An interesting feature of $\chi_\|$ is that the value at $T=0$ K is about 2/3 of that at T_N. In a normal antiferromagnet, the $\chi_\|$ becomes zero near $T=0$ K. In this system the Van Vleck paramagnetism does not appear because the first excited state

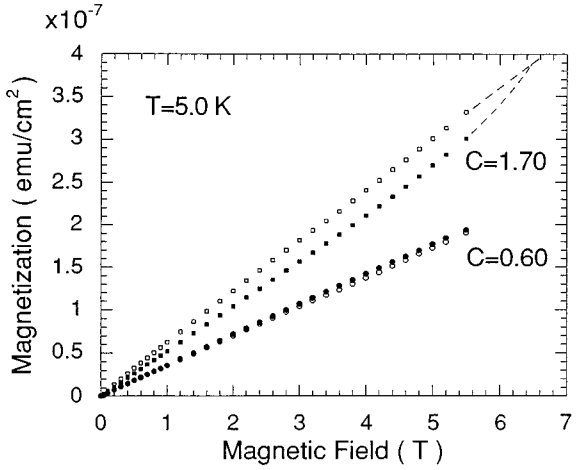

FIG. 4. The field dependence of the magnetization for the coverages $C=0.60$ (δ phase) and $C=1.70$ (ε phase) at $T=5.0$ K. The closed and open symbols correspond to the direction parallel and perpendicular to the Grafoil surface, respectively. The dashed lines are guides to the eyes.

is a singlet state and its energy is more than 10^4 K above the ground state. At this stage this phenomenon is not understood. One possibility is the effect of tilting of the molecular axis: the correction for the effect will reduce the value of $\chi_{\|}$. Another possibility is that another magnetic phase transition exists at a lower temperature.

C. Magnetization process

The magnetization (M) process at $T=5.0$ K for $C=0.60$ (δ phase) and 1.70 (ε phase) is shown in Fig. 4 by circles and squares, respectively. The open and closed symbols denote, respectively the magnetization in the field direction parallel [$M(H\|S)$] and perpendicular [$M(H\perp S)$] to the Grafoil surface. For $C=0.60$, $M(H\|S)$ and $M(H\perp S)$ are coincident with each other. However, for $C=1.70$ $M(H\|S)$ is smaller than $M(H\perp S)$ and $M(H\|S)$approaches to $M(H\perp S)$ at $T>3.0$ T. Figure 5 shows the field dependence of the differential susceptibility ($\Delta M/\Delta H\equiv D\chi$) obtained from the magnetization process of $M(H\|S)$ at $T=5.0$ K for the δ phase ($C=0.60$, 1.10), $\delta+\varepsilon$ phase ($C=1.50$), and ϵ

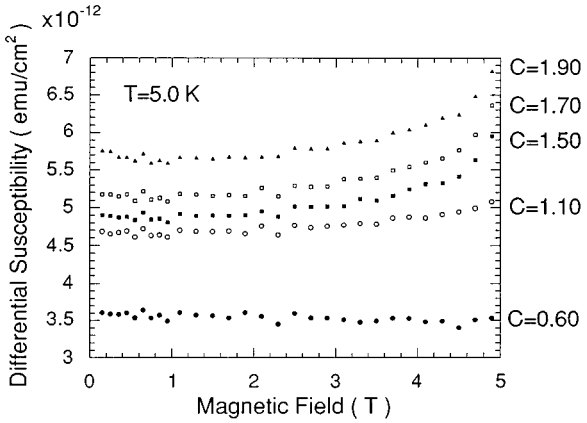

FIG. 5. The field dependence of the differential susceptibility for different coverages at $T=5.0$ K.

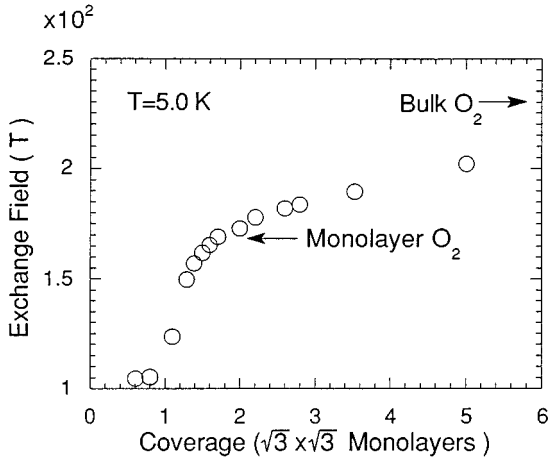

FIG. 6. The coverage dependence of the exchange field obtained from the magnetization process in the direction of the field perpendicular to the Grafoil surface at $T=5.0$ K.

phase ($C=1.70$, 1.90). The $D\chi$ for the δ phase is almost constant, while the $D\chi$ for the ε phase increases significantly above $H=3.0$ T. This increase of $M(H\|S)$ is considered as a precursor of the spin-flop transition. In bulk O_2 the spin-flop transition is observed at $H=6.9$ T ($T=4.2$ K).[1,2] From the observed tendency at high fields the spin-flop transition in the monolayer ε phase is estimated to occur between $H=6$ and 7 T. These results are another evidence of the magnetic long-range order in the ε phase.

The exchange field H_E is estimated by the formula

$$H_E=M_0/\chi_{\perp}, \tag{1}$$

where M_0 is the sublattice magnetization. The $\chi_{\perp}$ is obtained from the magnetization processes of $M(H\|S)$ and $M(H\perp S)$ by considering the mosaic structure of Grafoil. Figure 6 shows the coverage dependence of H_E assuming that $\chi_{\perp}$ can be approximated as $\chi(H\perp S)$. The H_E increases abruptly at coverages above $C=1.2$, where the ε phase is formed. With increasing coverage ($C\geqslant 1.7$), H_E increases linearly and approaches the value of bulk O_2 ($H_E=2.3\times 10^2$ T).[2] For the monolayer ε phase ($C=1.7$) the H_E is obtained as 1.7×10^2 T from Fig. 6. By considering the mosaic structure of Grafoil the true H_E is deduced as 1.6×10^2 T. Namely, H_E for the monolayer ε phase is reduced to about 70% of that for bulk O_2. The in-plane anisotropy field H_{D1} is estimated from the spin-flop field H_C by using a standard expression,

$$H_C=(2H_E\cdot H_{D1})^{1/2}. \tag{2}$$

Using the values of $H_E=1.6\times 10^2$ T and $H_C=6.5$ T, H_{D1} is obtained as 0.13 T. This value is almost the same as that of bulk O_2 ($H_{D1}=0.1$ T).[2]

D. Multilayer region

In this section we will describe the $\varepsilon-\zeta$ and melting transitions in the multilayer region. Figure 7 shows $\chi(H\|S)$ for some coverages at the $\varepsilon-\zeta$ transition. The magnitude of change of χ at the anomaly ($\Delta\chi$) increases until the coverage increases up to $C=1.70$, the coverage corresponding to

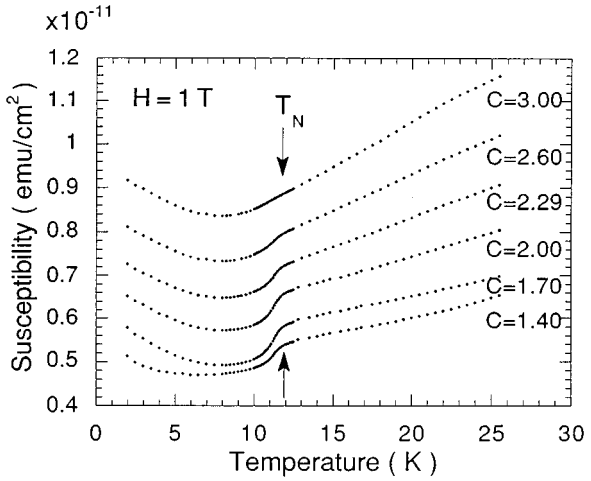

FIG. 7. Temperature dependence of $\chi(H\|S)$ near the $\varepsilon-\zeta$ magnetic transition temperature for different coverages ($H=1$ T).

the completion of the ε phase. As the coverage increases above $C=1.7$, the second layer grows, but the anomaly does not change significantly up to $C=2.0$. For $C>2.0$, $\Delta\chi$ decreases gradually and completely disappears at $C=2.8$, the coverage region corresponding to 65% of the full coverage of the second layer. This feature implies that the second layer has no contribution to the magnetic anomaly, but destroys the magnetic order of the first layer.

The whole features of the $\chi(H\|S)$ in the multilayer region are shown in Fig. 8. The $\chi(H\|S)$ and $\chi(H\perp S)$ show the same behavior above the $\varepsilon-\zeta$ transition temperature. The

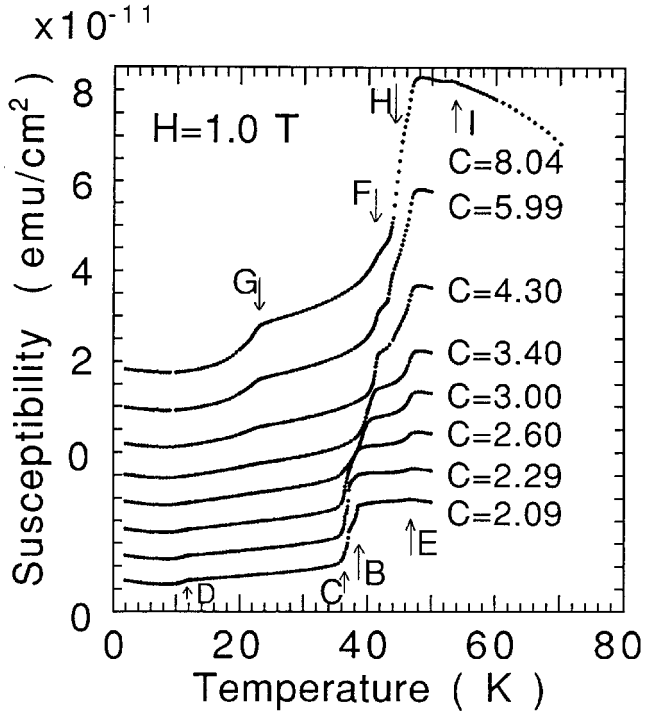

FIG. 8. Temperature dependence of $\chi(H\|S)$ in the O_2 multilayer coverage region ($H=1$ T). The arrows E, F, G, H, and I correspond to fluid-II–fluid-I transition temperature, the melting temperature of the third layer, the $\alpha-\beta$, the $\beta-\gamma$, and the γ-fluid transition temperatures of bulk O_2, respectively.

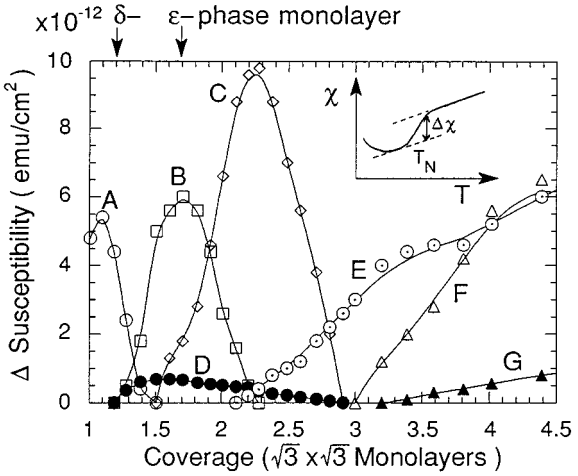

FIG. 9. Coverage dependence of the magnitude of change $\Delta\chi(H\|S)$ at $T=31.8$ K (A, open circles) 38.4 K (B, open squares), 37.0 K (C, open diamonds), 11.9 K (D, closed circles), 47.0 K (E, circles with dot), 41.5 K (F, open triangles), and 23.5 K (G, closed triangles), which correspond to the melting temperature of the δ phase, first layer, second layer (or first + second layer), the $\varepsilon-\zeta$ magnetic transition temperature, the fluid I-II transition temperature, the melting temperature of the third layer, and the $\alpha-\beta$ magnetic transition temperature of bulk O_2, respectively. The change at $\varepsilon-\zeta$ and $\alpha-\beta$ is taken as the difference at T_N between two lines drawn in the inset. Other changes are taken as follows: $\chi(31.8\text{ K})=\chi(32.0\text{ K})-\chi(31.6\text{ K})$, $\chi(38.4\text{ K})=\chi(38.5\text{ K})-\chi(38.0\text{ K})$, $\chi(37.0\text{ K})=\chi(37.2\text{ K})-\chi(36.4\text{ K})$, $\chi(47.0\text{ K})=\chi(47.0\text{ K})-\chi(46.0\text{ K})$, and $\chi(41.5\text{ K})=\chi(41.8\text{ K})-\chi(41.0\text{ K})$.

arrows B, C, and D indicate the meltings of the first and second layers for ζ phase, and the $\varepsilon-\zeta$ transition of the monolayer, respectively, similar to those in Fig. 1. The melting feature in the multilayer region $C>2.2$ is much different from those of the monolayer region. Increasing the coverage, the amplitude of anomaly B becomes smaller, while that of the anomaly C increases. At $C=2.29$ the anomaly B disappears and only the anomaly C remains; this means that the first and second layers melt simultaneously at $T=37.0$ K. As the coverage increases more, the anomaly associated with the melting becomes broad and shifts to a higher temperature. For $C>3.40$, which corresponds to the completion of the bilayer, the anomaly F is clearly observed at $T=41.5$ K, and the anomaly remains in the higher coverage region. The other anomaly E at $T=47.0$ K appear at $C=2.29$ and grows above $C=2.60$, which may be related to the transition between fluids I and II. These features will be discussed in Sec. IV C in relation with surface melting. We observe the formation of bulk O_2 above the coverage $C=3.40$; the anomalies G and H correspond to the magnetic phase transition ($\alpha-\beta$) and the structural phase transition ($\beta-\gamma$) of bulk O_2, respectively. The anomaly I at $C=8.04$ corresponds to melting of the γ phase of bulk O_2.

The coverage dependence of $\Delta\chi$ for structural and magnetic phase transitions is summarized in Fig. 9. The $\Delta\chi$ for the $\varepsilon-\zeta$ and $\alpha-\beta$ transitions is taken as the difference at T_N between the lines extrapolated from higher and lower temperatures, as shown in the inset of Fig. 9. In other cases the $\Delta\chi$ is the difference between the values at the temperatures just above and below the transition temperature. The

TABLE I. Exchange energy J and the mean-field ordering temperature estimated from lattice constants and susceptibility in the ε phase. a, b are lattice constants of a centered rectangular lattice, a_{NN} and b are nearest- and next-nearest-neighbor distances, respectively. J_{NN} and J_{NNN} are nearest- and next-nearest-neighbor interactions, respectively. The J_{NN} and J_{NNN} for ND are obtained from the distance between O_2 molecules using expression (4). The J_{NN} and J_{NNN} for χ are obtained from χ using expression (5). T_{MF} is the mean-field ordering temperature, T_N is the true magnetic transition temperature.

	Monolayer $C=1.94$ (ND) $T=4.5$ K (Ref. 12)	Monolayer $C=1.90$ (ND) $T=8.0$ K (Ref. 16)	Second layer $C=2.0$ (ND) $T=8.0$ K (Ref. 16)	Monolayer $C=1.70(\chi)$ $T=5.0$ K[a]	α phase of bulk O_2 $T=22.0$ K (Refs. 3 and 4)
a (Å)	5.463	5.471			5.403
b (Å)	3.410	3.390			3.433
a_{NN} (Å)	3.220	3.218	3.240		3.200
J_{NN} (K)	27.5	27.8	25.3	22.2	30.0
J_{NNN} (K)	12.2	13.3			11.0
T_{MF} (K)	114	112		82.9	130
T_N/T_{MF}	0.11	0.11		0.15	0.23

[a]Present work.

$\Delta\chi(A)$ for the melting temperature of the δ phase has a peak at $C=1.2$, the completion coverage of the δ phase, and disappears at $C=1.5$. In turn the $\Delta\chi(B)$ for melting of the first layer of the ζ phase increases, and the $\Delta\chi(D)$ for the $\varepsilon-\zeta$ transition also increases. The $\Delta\chi(B)$ and $\Delta\chi(D)$ saturate above $C=1.7$, which indicates the completion of the ζ monolayer phase. The close correlation of the coverage dependence of $\Delta\chi(B)$ and $\Delta\chi(D)$ implies that the magnetic phase transition occurs on the first layer of the ζ phase only. Above $C=1.7$ the second layer of the ζ phase begins to grow, but the magnitude of the magnetic anomaly does not increase beyond the saturation value of the first layer. This is more remarkable above $C=1.9$, where the second layer still grows, but the magnetic anomaly gradually decreases and completely disappears at $C=2.8$ as described above.

IV. DISCUSSION

A. Long-range ordering of the first layer

In Secs. III B and III C, we described that the first O_2 layer in the ε phase has long-range magnetic order. Our recent neutron-diffraction (ND) measurements[15,16] also show very clear evidence of the ordering, that is the observation of the magnetic Bragg peak below T_N. The magnetic coherence length is about 110 Å; the range of coherence is confined by the in-plane crystal size of Grafoil.

We describe the magnetic system of the ε phase with the spin Hamiltonian,

$$H=-2\sum_{\langle ij\rangle} J_{ij}S_i\cdot S_j-\sum_i D_1S_{xi}^2+\sum_i D_2S_{zi}^2. \qquad (3)$$

Here x and z axes are in the spin and molecular axis directions, respectively. The first sum runs over pairs $\langle ij\rangle$ of sites with a direct exchange interaction. In the present case, J_{ij} takes a constant value J_{NN} for four nearest neighbors, which are on the opposite magnetic sublattice, and J_{NNN} for the intrasublattice interaction with two next-nearest neighbors. The second and third terms are the small anisotropy terms which come from dipolar and molecular origin, respectively.[2,4] The value of J_{ij} is estimated as function of the distance between molecules as

$$J_{ij}=J_0\exp[-\alpha(r-r_0)], \qquad (4)$$

where $J_0=30.0$ K, $\alpha=4.30$ Å^{-1}, and $r_0=3.20$ Å .[2] Using the distance between O_2 molecules obtained from ND experiments[16] ($a_{NN}=3.218$ Å , $a_{NNN}=3.390$ Å), J_{NN} and J_{NNN} are estimated as 27.8 and 13.3 K, respectively. These value are not so different from those of bulk O_2, shown in Table I. Meanwhile, J_{NN} may be obtained from the observed value of $\chi_\perp$ using the expression from mean-field theory:

$$\chi_\perp=Ng^2\mu_B^2(1-\delta)/4|J|, \qquad (5)$$

where, $J=4J_{NN}$, $\delta\approx0.2$ includes the spin-wave correction and the ground-state energy correction.[2,4] Thus we obtain the experimental value $J_{NN}=22.2$ K, which is about 70% of that in bulk O_2 [J_{NN}(bulk)$=30$ K] as described in Sec. III C. The J_{NN} obtained in the present experiment is smaller than the calculated one from the distance dependence. This suggests that the reduction of J_{NN} may come from the substrate mediated interaction, which is inferred to be ferromagnetic. Actually, the $\varepsilon-\zeta$ transition is well reproduced by a Monte Carlo simulation by Duparc and Etters,[38–41] where the interaction of O_2-O_2, O_2-substrate-O_2, and O_2-substrate are considered in addition to the spin Hamiltonian (3). As shown previously in Fig. 3, the χ predicted from spin-wave theory for $J_{NN}=27.8$ K appears to agree with the observed $\chi_\perp$ better than the case for $J_{NN}=22.2$ K. However, the estimated value from the observed $\chi_\perp$ ($J_{NN}=22.2$ K) seems to be more reliable because the magnetic phase transition temperature for the monolayer is reduced to half of that of bulk O_2. Bulk O_2 is also regarded as a quasi-2D-system and the transition temperature is considered to be determined by the in-plane interaction.[2,4]

It is well known that the 2D Heisenberg model does not have long-range order at any finite temperature.[55] As this system is purely 2D, the $\varepsilon-\zeta$ magnetic phase transition is considered to be realized by a small anisotropy in expression (3). In quasi-2D magnets, the magnetic transition takes place well below the mean-field ordering temperature,

$$T_{\mathrm{MF}}=2S(S+1)z|J|/3. \tag{6}$$

A DeJong-Miedema survey shows that quasi-2D magnets have T_N/T_{MF} in the range 0.36–0.48.[56] As shown in Table I, an O_2 monolayer has a very small value of T_N/T_{MF} even though that of bulk O_2 is already small. T_N means the true magnetic transition temperature when the $\varepsilon-\zeta$ transition does not intervene. The reason may be attributed to the reduction of the thermal average $\langle S\rangle$ of the O_2 spin. According to our recent ND experiments,[15,16] the value of $\langle S\rangle$ extrapolated to $T=0$ K is 0.61 ± 0.09: the reduction is 39%. This reduction is very large compared with the experimental and theoretical values for the 2D Heisenberg system, in which the reduction is 20–25 % due to the zero-point quantum fluctuation.[57,58]

The change of χ just below T_N, in our measurements, is continuous. This seems to be consistent with the previous ND result, which gives a continuous transition.[12] However, Mochrie *et al.* observed the coexistence of the ε and ζ phases between 11.1 and 11.9 K.[9] So, the present observed continuous change of χ in the temperature region may be attributed to the coexistence of ε and ζ phases. In the previous heat-capacity measurement, two successive phase transitions are reported by Marx and Christoffer, who concluded that the first one is a three-state Potts transition with the lattice distortion at $T=11.65$ K, and the second is an Ising transition from the paramagnetic to the antiferromagnetic state at $T=11.32$ K.[24] However, our χ measurements do not show any evidence of the two phase transitions. The observed transition temperature ($T_N=11.9\pm0.1$ K), which is determined as the temperature of the separation of $\chi(H\|S)$ and $\chi(H\perp S)$, is close to the upper temperature observed by Marx *et al.* In our recent ND results,[15,16] the magnetic Bragg peak is observed even at $T=11.5\pm0.05$ K, which is not consistent with Marx's model. So, our results support Mochrie's suggestion, that is, the two transitions observed by Marx *et al.* are connected with the entry and exit from the two-phase coexistence region in a heterogeneous substrate.

B. Magnetic ordering of second oxygen layer

In the coverage region $C>1.7$, the second O_2 layer grows on top of the first layer. As described in Sec. III D, we observed that the amplitude of the anomaly at T_N has a maximum at $C=1.7$, and decreases gradually with increasing coverage. This means that the first layer is responsible for the magnetic transition but the second layer does not contribute to it. This result is confirmed by our recent ND measurements: the magnetic diffraction intensity is not increased in the coverage region $C>1.7$, and the nuclear peak of the second layer is not split below T_N which means the second layer is not deformed, though the integrated intensity of the second layer is increased.[15,16] The magnetic disorder state of the second layer is very curious because we observed a clear diffraction peak of the second layer in the ND experiments, and the structure of the second layer is almost the same regular triangular lattice above T_N: a_{NN} (second) = 3.23 Å, a_{NN} (first) = 3.28 Å at $T=15.0$ K, $C=2.0$.[16] The difference of the magnetic ordering between first and second layers may be considered to be the effect of the substrate. However, the effect of the substrate would decrease the antiferromagnetic interaction between O_2 molecules as discussed in Sec. IV A.

A possible explanation is a random field effect. It is well known that the ordered state in a 2D magnet is unstable under an arbitrary weak random field, which is conjugate to the order parameter.[59,60] This effect is also experimentally observed in diluted magnets.[61–63] The O_2 molecules in the second layer feel an exchange field from magnetically ordered O_2 in the first layer. As the O_2 second layer is incommensurate with the first layer, the amplitude and direction of the exchange field is not the same for each O_2 molecule in the second layer. If the exchange field is regarded as a random field, the magnetic order of the second layer may be destroyed. The decrease of the anomaly at T_N with the increase of the second layer coverage may be also explained by a random field effect. The O_2 molecules in the first layer also feel the random exchange field from the magnetic moment of O_2 in the second layer, which is induced by an applied static field. As shown in Fig. 9, the magnetic order is almost destroyed at coverages higher than $C=2.8$, which corresponds to 65% of the full coverage of the second layer. At this coverage, the second layer has structural long-range order, because the site percolation concentration in the 2D triangular lattice is 0.500. Namely, as all O_2 molecules in the first layer feel the random field from the second layer at this coverage, the magnetic order of the first layer may be almost destroyed. According to this model we should observe the recovery of the first layer ordering in zero magnetic field, because the induced moment from O_2 molecules in the second layer is zero. Actually, in our recent ND experiment in zero magnetic field, the magnetic diffraction peak intensity at $C=2.62$ is almost the same as that at $C=1.78$.[16]

C. Melting features in multilayer regions

As described in Sec. III D, the melting in a multilayer region is complicated, but we can understand it qualitatively as follows. In the coverage region $C=1.6$–2.2, we observed two melting transitions of the first and second layers at different temperatures $T=38.4$ and 37.0 K, respectively, that is, there is a phase consisting of a solid first layer and a liquid second layer (η phase). For $C=2.2$–2.9, the melting temperatures coincide with each other at $T=37.0$ K, which means that the melting temperature of the first layer becomes the same temperature as that of the second layer. When the second layer melts, the liquid of the second layer gives a random van der Waals force to the first layer. At the coverage of the second layer of 30% ($C=2.2$) of the full one, the first layer cannot remain as a solid due to a strong force from the melted second layer. Namely, above this coverage the first and second layers melt simultaneously.

The melting feature in the much higher region is well shown in $\chi(H\|S)$ for $C=4.30$ of Fig. 8, in which the anomalies at $T=41.5$, 45, and 47 K are observed. These can be understood in terms of surface melting as proposed by Krim *et al.*[13,14] They observed that the ND diffraction peak of a

TABLE II. Melting temperatures in a multilayer region.

T_{melt} (K)	37.0	38.4	41.5	~44.5	47
$C=1.6–2.2$	Second layer	First layer			
$C=2.2–2.9$	First and second layer				
$C=3.4–$			Third	Second layer	First layer

solid remains in the fluid II ($41.5<T<47.0$ K): the fluid II results from surface melting and the surface-melted component reaches that of the film itself at $T=47.0$ K. According to Krim's scheme the anomalies at $T=41.5$, 45, and 47 K correspond to the melting of the third, second, and first layers, respectively. These melting temperatures are summarized in Table II. However, the melting feature around $C=3.00$ is not understood enough at present. It shows a broad change of $\chi(H\|S)$ between $T=37.0$ and 40.0 K with a small anomaly at $T=47$ K.

V. CONCLUSION

We measured the magnetic susceptibility and magnetization process of O_2 monolayers and multilayers physisorped on exfoliated graphite. The following results are elucidated.

(1) In the dense monolayers phase (ε phase), the antiferromagnetic anisotropy of χ has been observed below $T_N=11.9\pm0.1$ K.

(2) The magnetic-field dependence of $\chi(H\|S)$ in the ε phase shows the precursor of the spin-flop transition, which is estimated at a field of $6<H<7$ T at $T=5.0$ K.

The results of (1) and (2) confirm the existence of magnetic long-range order in the ε phase, which is a purely 2D Heisenberg antiferromagnetic phase with a small anisotropy.

(3) In the fluid II of the dense monolayer region, the O_2 molecules have orientational order.

(4) The nearest-neighbor magnetic interaction between O_2 molecules in the dense monolayer is reduced to 70% of that of bulk O_2, which may be due to a substrate mediated interaction.

(5) In the bilayer region, the second layer is not ordered magnetically, and the magnetic ordering of the first layer is destroyed when the coverage of the second layer amounts to 65% of the full coverage of the second layer. This result may be attributed to a random-exchange field effect between the first and the second O_2 layers, which are incommensurate to each other.

(6) In the multilayer region, features of the melting transition can be understood in terms of surface melting.

ACKNOWLEDGMENTS

We gratefully acknowledge Professor D. Guerard for furnishing the sample of vermicular graphite. The present work was supported by Grant-in-aid for Scientific Researches from the Ministry of Education, Science and Culture.

*Present address: Photon Factory, National Laboratory for High Energy Physics, Oho, Tsukuba, Ibaraki 305, Japan.

[1] R. J. Meier, C. J. Schinkel, and A. de Visser, J. Phys. C **15**, 1015 (1982).
[2] C. Uyeda, K. Sugiyama, and M. Date, J. Phys. Soc. Jpn. **54**, 1107 (1985).
[3] R. J. Meier and R. B. Helmholdt, Phys. Rev. B **29**, 1387 (1984).
[4] P. W. Stephens and C. F. Majkrzak, Phys. Rev. B **33**, 1 (1986).
[5] M. Drir and G. B. Hess, Phys. Rev. B **33**, 4758 (1986).
[6] H. S. Youn and G. B. Hess, Phys. Rev. Lett. **64**, 443 (1990).
[7] P. W. Stephens, P. A. Heiney, and R. J. Birgeneau, Phys. Rev. Lett. **45**, 1959 (1980).
[8] P. A. Heiney, P. W. Stephens, S. G. J. Mochrie, J. Akimitsu, R. J. Birgeneau, and P. M. Horn, Surf. Sci. **125**, 539 (1983).
[9] S. G. Mochrie, M. Sutton, J. Akimitsu, R. J. Birgeneau, P. M. Horn, P. Dimon, and D. E. Moncton, Surf. Sci. **138**, 599 (1984).
[10] K. Morishige, K. Mimata, and S. Kittaka, Surf. Sci. **192**, 197 (1987).
[11] J. P. McTague and M. Nielsen, Phys. Rev. Lett. **37**, 596 (1976).
[12] M. Nielsen and J. P. McTague, Phys. Rev. B **19**, 3096 (1979).
[13] J. Krim, J. P. Coulomb, and J. Bouzidi, Phys. Rev. Lett. **58**, 583 (1987).
[14] R. Chiarello, J. P. Coulomb, J. Krim, and C. L. Wang, Phys. Rev. B **38**, 8967 (1988).
[15] Y. Murakami, I. N. Makundi, T. Shibata, H. Suematsu, M. Arai, H. Yoshizawa, H. Ikeda, and N. Watanabe, Physica B **213&214**, 233 (1995).
[16] I. N. Makundi, Doctor thesis, University of Tokyo, 1993.
[17] S. Gregory, Phys. Rev. Lett. **40**, 723 (1978).
[18] D. D. Awschalom, G. N. Lewis, and S. Gregory, Phys. Rev. Lett. **51**, 586 (1983).
[19] U. Köbler and R. Marx, Phys. Rev. B **35**, 9809 (1987).
[20] H. Suematsu and Y. Murakami, J. Magn. Magn. Mater. **90&91**, 749 (1990).
[21] Y. Murakami and H. Suematsu, Surf. Sci. **242**, 211 (1991).
[22] J. Stoltenberg and O. E. Vilches, Phys. Rev. B **22**, 2920 (1980).
[23] R. Marx and R. Braun, Solid State Commun. **33**, 229 (1980).
[24] R. Marx and B. Christoffer, Phys. Rev. Lett. **51**, 790 (1983).
[25] R. Marx and B. Christoffer, Phys. Rev. B **37**, 9518 (1988).
[26] M. F. Toney, R. D. Diehl, and S. C. Fain, Jr., Phys. Rev. B **27**, 6413 (1983).
[27] M. F. Toney and S. C. Fain, Jr., Phys. Rev. B **30**, 1115 (1984).
[28] H. You and S. C. Fain, Jr., Phys. Rev. B **33**, 5886 (1986).
[29] M. F. Toney and S. C. Fain, Jr., Phys. Rev. B **36**, 1248 (1987).
[30] M. Bienfait, J. L. Seguin, J. Suzanne, E. Lerner, J. Krim, and J. G. Dash, Phys. Rev. B **29**, 983 (1984).
[31] J. A. Venables, J. L. Seguin, L. Suzanne, and M. Bienfait, Surf. Sci. **145**, 345 (1984).
[32] E. T. Jensen, R. E. Palmer, and P. J. Rous, Phys. Rev. Lett. **64**, 1301 (1990).
[33] E. T. Jensen and R. E. Palmer, Surf. Sci. **237**, 153 (1990).
[34] J. C. Barnard, K. M. Hock, L. Siller, M. R. C. Hunt, J. F. Wendelken, and R. E. Palmer, Surf. Sci. **291**, 139 (1993).

[35] W. Eberbardt, and E. W. Plummer, Phys. Rev. Lett. **47**, 1476 (1981).
[36] A. Nilsson, R. E. Palmer, H. Tillborg, B. Hernnäs, R. J. Guest, and N. Mårtensson, Phys. Rev. Lett. **68**, 982 (1992).
[37] H. Tillborg, A. Nilsson, B. Hernnäs, and N. Mårtensson, Surf. Sci. **295**, 1 (1993).
[38] R. E. Palmer, P. J. Rous, J. L. Wilkes, and R. F. Willis, Phys. Rev. Lett. **60**, 329 (1988).
[39] P. J. Rous, R. E. Palmer, and R. F. Willis, Phys. Rev. B **39**, 7552 (1989).
[40] R. J. Guest, A. Nilsson, O. Björneholm, B. Hernnäs, A. Sandell, R. E. Palmer, and N. Mårtensson, Surf. Sci. **269/270**, 432 (1992).
[41] R. D. Etters, R. P. Pan, and V. Chandrasekharan, Phys. Rev. Lett. **45**, 645 (1980).
[42] R. P. Pan, R. D. Etters, K. Kobashi, and V. Chandrasekharan, J. Chem. Phys. **77**, 1035 (1982).
[43] R. D. Etters and O. M. B. Duparc, Phys. Rev. B **32**, 7600 (1985).
[44] O. M. B. Duparc and R. D. Etters, J. Chem. Phys. **86**, 1020 (1987).
[45] K. Flurchik and R. D. Etters, J. Chem. Phys. **84**, 4657 (1986).
[46] S. Tang, S. D. Mahanti, and R. K. Kalia, Phys. Rev. Lett. **56**, 484 (1986).
[47] Y. P. Joshi and D. J. Tildesley, Surf. Sci. **166**, 169 (1986).
[48] Grafoil is purchased from Union Carbide Corp.
[49] The vermicular graphite is a preproduct of Papyex, which is made by Le Carbon Lorraine.
[50] R. J. Birgeneau, P. A. Heiney, and J. P. Pelz, Physica B **109&110**, 1785 (1982).
[51] S. Brunauer, P. H. Emmett, and E. Teller, J. Am. Chem. Soc. **60**, 309 (1938).
[52] A. C. Mota, Rev. Sci. Instrum. **42**, 1541 (1971).
[53] The anisotropy of χ was not observed in our previous χ measurements (Refs. 20 and 21). This may be ascribed to the quality of the monolayer crystal, which depends on the annealing time after adsorption.
[54] M. Takahashi, Phys. Rev. B **40**, 2494 (1989).
[55] N. D. Mermin and H. Wagner, Phys. Rev. Lett. **17**, 1133 (1966).
[56] L. J. deJongh and A. R. Miedema, Adv. Phys. **23**, 1 (1974).
[57] E. Manousakis, Rev. Mod. Phys. **63**, 1 (1991).
[58] R. R. P. Singh, Phys. Rev. B **41**, 4873 (1990).
[59] Y. Imry and S. K. Ma, Phys. Rev. Lett. **35**, 1399 (1975).
[60] A. Aharony, Solid State Commun. **28**, 667 (1978).
[61] S. Fishman and A. Aharony, J. Phys. C **12**, L729 (1979).
[62] H. Yoshizawa, R. A. Cowley, G. Shirane, R. J. Birgeneau, H. J. Guggenheim, and H. Ikeda, Phys. Rev. Lett. **48**, 438 (1982).
[63] R. J. Birgeneau, H. Yoshizawa, R. A. Cowley, G. Shirane, and H. Ikeda, Phys. Rev. B **28**, 1438 (1983).